Journal Home Page: https://sites.google.com/a/univsul.edu.iq/sjes

Review Article:

In-plane Shear Strengthening of Masonry Walls after Damage

Ahmed Mohamed Raouf[1]
Jalal Ahmed Saeed[1]

[1]University of Sulaimani, College of Engineering, Civil Engineering Department

Article Inform

Article History:
Received 15 July 2019
Accepted 28 August 2019
Available online 1 April 2020

Keywords: Damaged wall, In-plane loading, Masonry wall, Shear strength, strengthening materials.

About the Authors:
Corresponding author:
Ahmed Mohamed Raouf - MSc.
E-mail: ahmedrauf91@gmail.com
Researcher Involved:
Dr. Jalal Ahmed Saeed – Professor

DOI Link: https://doi.org/10.17656/sjes.10122

Abstract

This study investigates the effect of 5 different strengthening materials on damaged Un-Reinforced Masonry (URM) brick walls under an in-plane lateral loading and a predefined uniform vertical load. Five clay brick walls with a dimension of (1200 × 935 × 115) mm were tested then strengthened with plastic mesh, glass fiber mesh, steel mesh, wild cane strips, and chopped steel fibers. The walls were tested again up to failure in order to determine the best material in terms of shear strength and ductility. Two more walls were tested similarly without strengthening to serve as control walls. Based on the experimental results, GM-r (strengthened with glass fiber mesh) had the highest ductility factor of 23.2 and showed the best strength retention amongst the strengthened walls. OG-r (strengthened with wild cane grid) had the highest toughness ratio value of 10.1 even though it is not suitable for exterior walls due to biological factors such as rotting and incompatibility with high moisture areas. SM-r (strengthened with steel mesh) retained 89% of the damaged wall and at the same time inadequate in seismic areas due to its sudden brittle de-bonding failure. Walls PM-r and SF-r lacked strength and ductility retention, respectively, to be considered as a feasible option in sustaining lateral loads.

1. Introduction

Masonry is a type of construction that is widely practiced around the world similar to concrete and steel. Brick masonry and masonry in general, provide numerous functions including and not limited to structural support, sub division of space, thermal insulation, and weather protection. Un-Reinforced Masonry (URM) structures are often sufficient in sustaining gravity loads; however, they are inadequate when subjected to lateral forces (i.e. seismic forces) that are transferred from the diaphragm to the foundation through the walls by in-plane action [1]. Failure of the unreinforced in-plane walls is therefore anticipated due to the walls inherent brittle nature and limited tensile/shear strength.

In most cases, the aspect ratio (L/H) of the wall dictates the possible modes of failure which can be described as flexural cracking, rocking followed by toe crushing, shear sliding, and diagonal tension cracking [2]. There are a few engineering solutions for such a problem, but rehabilitation, rather than reconstruction, of the damaged walls is preferred when cost and implementation are taken into consideration.

Therefore, strengthening of URM walls has been the main focus of researchers for many years.

Many materials and methods have been used to strengthen as-built URM walls (prior to damage). Traditional surface treatment methods in general, which encompasses ferro-cement jacketing, reinforced plaster, and shotcrete have been successfully used in the past where it has increased in-plane ductility, stiffness, shear strength, and crack resistance capacity [3-6].

Other methods such as Near Surface Mount (NSM), which includes making a groove on the surface of the wall and inserting reinforcement, has been investigated and proved to be effective in increasing the in-plane shear strength, deformation capacity, and ductility of the walls[7,8].

Moreover, other distinctive materials and methods such as Textile Reinforced Mortar (TRM), bamboo, hemp fibers, and Inorganic Matrix-Grid (IMG) composites have been used by various researchers and have shown promising improvement in shear strength and ductility[9-12]. More recently, Fiber Reinforced Polymer (FRP) has been the interest of researchers due to its many beneficial factors such as its high strength to weight ratio, fast application rate, low maintenance, easy handling etc.[13].

Repairing of URM walls after they have been damaged has also been studied as part of a broader investigation on URM wall strengthening. Materials and methods such as FRP and NSM have been used as a repairing mechanism and have shown considerable enhancement in shear strength, energy dissipation, and ductility[14-16].

Weng et al.[14], ElGawady et al.[15], Konthesingha et al. [16], and Santa-Maria and Alcaino [17], have all studied the effects of repairing damaged masonry walls with FRP and their main conclusions were that FRP can effectively improve the integrity of the masonry walls up to similar deformation values as the undamaged strengthened walls and that the retrofitted walls had similar improvements in behavior irrespective of the amount of damage previously sustained.

This study adds to the existing literature by considering various materials other than FRP that are easily available, then specifically applying them for strengthening previously damaged URM walls. The materials that were used in this study were plastic mesh, glass fiber mesh, steel mesh, organic (wild cane) grid, and chopped steel fiber which were all covered with a cement plaster, or mixed with cement plaster in the case of steel fiber.

1.1. Research objectives

The aim of this study is to investigate the behavior and shear strength of the strengthened damaged masonry walls. The specific objectives are as follows:

1- Compare the type of materials that are used to strengthen the damaged wall in terms of shear strength, ductility, and toughness.
2- Determine the best material (among the selected) that could be used for shear strengthening of the damaged wall.

2. Experimental program

2.1. Test specimens

The experimental program consisted of constructing, testing, strengthening, and retesting 5 clay brick masonry walls with a dimension of (1200 × 935 × 115) mm (aspect ratio of 1.28) under static gradual lateral loading and a predefined vertical compression.

The walls were tested until a crack was observed, strengthened with specific materials on one face, and tested again up to failure. Additionally, two walls (plain and cement plastered) were constructed and tested up to failure to serve as control walls.

The designation of the walls is as follows; the letter "C" is for the plain control wall without any

type of strengthening. "PL" represents the cement plastered control wall. The designation used for the walls that are tested before strengthening are the same for those that are strengthened except for the letter "r".

The first letter is the material name while the second letter represents the orientation/location or type of material used. The letters "S", "G", and "M" represent Steel, Grid (or Glass when used as the first letter), and Mesh, respectively. The designation of the walls and strengthening methods are summarized in Table 1. The variables in the testing program were the type of strengthening and techniques used.

2.2. Material properties

Ordinary Portland Cement Type I Tasluja cement, Darbandixan natural fine aggregate (S.G. = 2.56) and natural coarse aggregate (S.G. = 2.69) with a maximum size of 12 mm were used for casting the beams which were placed under and on top of the specimens. Moreover, steel reinforcement bars of 6mm diameter (f_y = 312 MPa) were used for the beams.

The concrete mix design for the beams yielded a ratio of (1: 2.4: 2) (cement: fine agg.: coarse agg.) with a w/c ratio of 0.62 and an average cube compressive strength of 37.52 MPa. The same cement and fine aggregate were used for the masonry mortar, the cement plastering mortar, and the repairing mortar. Locally manufactured clay bricks, made by "Aso Brick Factory" in Sulaimaniyah-Iraq, having a nominal dimension of (235 × 115 ×75)mm were used.

The mechanical properties of the materials are summarized in Table 2.

2.2.1. Strengthening materials

The properties of the strengthening materials such as tensile strength and weight are summarized in Table (3). Additionally, a photograph of each material is shown in Fig.1.

A polypropylene plastic mesh with a clear opening size of (13.6 × 10) mm was used. Each single wire comprising the mesh had a rectangular cross section of (1.3 × 1.1) mm as shown in Fig.1-a. The ultimate tensile strength was 16.57 MPa based on laboratory testing of a single wire. The welded wire steel mesh had an opening size of (11.25 × 11.25) mm and a diameter of 1.50 mm as shown in Fig.1-b. The ultimate tensile strength of the steel mesh was 303 MPa based on laboratory testing of a single wire.

Glass fiber mesh, with uni-directional roving, was used with a nominal spacing of 4.2mm between roving. Each roving was 1.5 mm wide with a fiber area of 0.15 mm^2 in the main direction. The clear spacing between roving was 4.7 mm in the main and transverse direction as shown in Fig.1-c. The ultimate tensile strength of the glass fiber was 238.7 MPa based on testing an individual fiber.

A natural Arundo donax, more commonly known as wild cane, was obtained locally from Qaradagh district, Sulaimaniyah-Iraq. The average inner and outer diameter of the cane was 12.6mm and 17.2mm, respectively. The cane was cut, using a power saw, longitudinally into equal strips with an average width of 10mm. The strips were made into a grid with orthogonal directions putting the horizontal strips first and the vertical strips afterwards which were tied together using steel wire ties. The opening size of the grid was (40 × 40) mm as shown in Fig.1-d. The ultimate tensile strength of the cane was 94 MPa based on the "yuksel kaya makina" tensile testing machine at Seko laboratory, Sulaimaniyah.

The steel fibers were made from a woven steel wire mesh that was manually chopped using a metal cutter. The mesh was cut into smaller strips and then chopped into fibers as shown in Fig.1-e. The diameter of the steel fiber was 0.5 mm and the average aspect ratio was 50 depending on the chopped length. Due to the woven state of the mesh, the resulting steel fibers had a crimp-like shape. The ultimate tensile strength of the chopped steel fiber was 418 MPa based on laboratory testing of the wire before chopping.

2.3. Construction process

A total of 14 reinforced concrete beams with a dimension of (1200 × 115 × 105) mm were cast in order to be placed below and on top of the wall specimens. The R.C. beams consisted of 4 steel bars of 6mm diameter placed longitudinally in order to satisfy the minimum requirement for flexure and 6mm diameter steel bars for the ties which were spaced at 250 mm c/c to keep the longitudinal bars in position. The bottom beam provides a level surface for the construction of the wall while the top beam further distributes the vertical load. These beams represent floor levels in actual practice.

The wall specimens, including the control walls, were constructed with mortar (1:3) of (cement: sand) by weight and about 10 mm horizontal and vertical joint thickness using a stretcher bond layout. The wall construction started with putting the previously prepared bottom R.C beam then building the wall on top of the beam until the necessary height was achieved. The top R.C beam was placed with same mortar mix on top of the wall the following day.

Some of the walls had steel tie wires placed at specified intervals to hold the strengthening materials in place. The final dimension of the walls was (1200 × 1155 × 115) mm including the beams. The details of the tested specimens are shown in Fig.2. The walls were moist cured for 14 days at least and left for about 2 months before testing. All the strengthened specimens were painted with white paint (emulsion paint: chalk powder) for better appearance of crack pattern. The cement plastered control wall was constructed identically as the other walls aside from a 10mm 1:3 (C: S) cement plastering of the walls surface.

2.4. Strengthening procedure

Subsequent to the walls testing, all the damaged walls (except the control walls) were wetted and their cracks were repaired, as much as possible, with 1:2 (C: S) mortar using a trowel. For walls "PM" and "GM", a thin layer of about 5mm was cement plastered and then a 40cm wide mesh was placed first diagonally across the crack and later a second layer, covering the entire wall, was placed.

Both meshes (diagonal and full surface covering) were tied to the wall by the steel tie wires that were placed at specified locations (two at every horizontal joint) earlier during construction of the wall. A second layer of cement plastering, about 10mm, was applied covering the mesh and resulting in a total thickness of about 15mm cement plaster.

The same procedure was performed for wall "SM" except that only one mesh (covering the whole surface) was applied. For wall "OG", one grid was applied and the total thickness was 20mm due to the thickness of the overlapping canes. Finally, for wall "SF", a 10 mm cement plaster, mixed with 1.5% steel fiber (of total mortar volume), was applied. The strengthened walls are shown in Fig. 3.

2.5. Test setup and testing procedure

A steel frame was specially manufactured for this research which consisted of a rectangular self-balanced closed frame with internal dimensions of 2200 mm by 2000 mm in length and height, respectively. A long steel rectangular plate (15 × 100) mm was welded on the frame diagonally to prevent sway of the frame as shown in Fig. 4-1. Two steel plates (300 × 400 × 10) mm and 4 steel bolts were used to fix the vertical and lateral applying hydraulic hand operated jacks to their designated locations as shown in Fig.4-2. The vertical jack Fig.4-3. having a 30 ton capacity, included a pressure gauge and was fixed on top of the beam to apply a predefined pre-compression load on to the wall through 3 steel beams (steel box (100 × 100 × 4) mm with strengthened sides to prevent web buckling).

The beams were supported on round bars Fig. 4-4 which allowed free horizontal movement of the wall and were placed on an 8mm steel plate placed on top of the upper R.C beam of the wall. The lateral jack Fig.4-5 having a 50 ton capacity, was fixed horizontally to apply the lateral load during testing. A vertical link Fig.4-6 was provided at

the edge of the wall near the horizontal load assembly.

The link consisted of two rectangular steel bars (40 × 15) mm hinged at the bottom with the beam of the frame and connected at top with a 40 mm pin supported on steel plate which in turn was supported on 4 round bar rollers. This link prevented the wall from overturning and allowed the wall to move horizontally because of the presence of the rollers and the top pin.

The wall specimen was placed on the bottom beam (member) of the steel testing frame, a steel plate 8mm thick was put on top beam of the wall, 7 rollers of 25mm diameter were put between the steel plate and the distributing steel beam to convert the vertical point load to a uniformly distributed point load on the wall as well as allow unrestricted lateral displacement.

A load was applied by the vertical jack generating a constant stress of 0.33 MPa pre-compression on the wall. Afterwards, the horizontal load was applied gradually up to failure in increments of 20 bars (15kN) while simultaneously recording both horizontal and bottom dial gauges at every load increment.

The horizontal displacement of the wall was measured at the center of the top R.C beam of the tested wall in the direction of the lateral load on the same line of action using a digital dial gauge Fig.4-7 with 0.001mm accuracy. The vertical displacement of the wall (from overturning) was measured by a dial gauge Fig. 4-8. with 0.01mm accuracy placed on the bottom R.C beam at the base of the wall on the horizontal load side.

3. Results and discussion

3.1. Failure mechanism

Results of the tested specimens are shown in Table (4). The failure mode of the un-strengthened walls (C, PM, GM, SM, OG) was an explosive sudden shear failure at the peak load. The shear crack extended from the loading corner (left side) towards the compression corner (right side) and passed diagonally through both the brick and the mortar as shown in Fig.5-a.

The crack followed such a route most likely due to the high strength of the mortar as well as the aspect ratio of the wall. The failure pattern of "PL", cement plastered wall, also exhibited a sudden shear failure, however, unlike the other walls, the path of the diagonal crack passed through the bed and head joints (stepwise manner) instead of the brick and mortar as shown in Figs. 5-b and 5-c.

Wall "SF" exhibited the same mode of failure as the others except that the diagonal shear failure developed near the middle of the wall (top side) and towards the compression corner as shown in Fig.6-a. It is important to note that the control walls C and PL were tested beyond their peak load to determine their shear strength and ductility after their initial explosive shear crack.

It was established that the control walls did not attain any ductility and that any residual strength remaining in the wall was due to the pre-compression of the vertical jack. Moreover, the failure nature of all the tested walls before strengthening were very similar to the control walls and thus the strengthened walls will be compared and contrasted with their original tested selves instead of the control walls.

The failure mode of the strengthened walls was different in nature when compared to those of the un-strengthened walls. Wall "PM-r" (strengthened with plastic mesh) exhibited a diagonal shear failure when the peak load was reached at 134.6 kN (43% of PM) as shown in Fig.6-e. At the peak load, a sudden drop (39%) of the load carrying capacity was observed and a sudden crack emerged from a point close to the previous crack origin (PM) and followed the old crack path towards the compression corner.

Loading was applied after the peak load which gradually widened the existing diagonal crack, caused the plaster at the compression corner to de-bond at 82.26 kN (61% of post peak strength), and reduced the load carrying capacity of the wall. After further loading, the rupture of the plastic mesh was observed at 56.1 kN (42% of post peak strength) as shown in (Fig. 6-f) and a 20% drop in strength was observed. Continued loading only widened the existing crack with no apparent extra resistance from the wall.

For wall "GM-r" (strengthened with glass fiber mesh), thin diagonal cracks appeared at earlier

loads equivalent to 84% and 95% of the peak load before eventually reaching the peak load at 142.1 kN (68% of GM) as shown in Fig.7-b.

There was a drop (37%) in load carrying capacity at the peak load and the diagonal cracks softly propagated towards the bottom of the wall but did not follow the same path as those of the original wall (GM). However, the plain side (backside) of the wall revealed that the cracks did in fact follow the original crack path (from GM) as shown in Fig.7-c. This is probably due to the plaster de-bonding at the right part of the wall. The continued load after the peak load caused gradual widening of the cracks, further gradual load drops, and rupture of the mesh fibers.

For wall "SM-r" (strengthened with steel mesh), numerous thin diagonal short cracks (energy dissipation) appeared at the peak load (254.24 kN or 89% of SM) as shown in Fig.7-e and when loading continued to be applied, the load did not increase but a loud sudden brittle de-bonding of the reinforced plaster (without yielding of the steel mesh) took place resulting in a huge drop (70%) in the load carrying capacity as shown in Fig.7-f.

The steel mesh caused a different diagonal path (as opposed to SM) on the wall as was revealed from the plain side as shown in Fig.7-g. The continued loading after failure only further separated the two diagonal parts of the wall behind the reinforced mesh.

For wall "OG-r" (strengthened with wild cane grid), thin diagonal cracks appeared at 164.5 kN (85% of peak load) as loading was increased until the peak load was reached (194.4 kN or 81% of OG) and a drop (12%) of the load carrying capacity to 172 kN was observed.

When loading was continued, the existing cracks quickly propagated towards the compression corner, rupture of the strands was heard, and a larger drop of strength (30% from the 172kN) was observed. With further loading, four resulting major diagonal parallel cracks occurred from the loading corner towards the compression corner as shown in Fig.7-i.

The plain side also showed that despite the visible cracks resulting on the strengthened side, the wall failed through the original crack (from OG) as shown in Fig.7-j.

Wall "SF-r" (strengthened with steel fiber) showed the worst outcome out of the strengthened walls. The strengthening did not allow the development of any cracks until the peak load was reached at 134.6 kN (47% of SF). At the peak load, a sudden brittle diagonal shear failure occurred at the same location as the previous crack (SF). The failure behavior of SF-r was similar to the failure behavior of SF shown in Fig.6-a since both walls could not sustain any extra loading after the peak load was reached. Continued loading only separated the walls further without any resistance.

3.2. Load-lateral deflection behavior

All the un-strengthened walls exhibited a fairly linear relationship up to the peak point (ultimate load) followed by an abrupt reduction in lateral load capacity with a sudden gain in horizontal displacement due to the explosive diagonal shear failure. The walls were brittle in nature and no residual strength or ductility was observed as shown in the dash lines of Fig.8-a to Fig.8-e.

The strengthened walls generally displayed similar load-lateral deflection behaviors. First, the slope of the graph showed an almost linear behavior until the peak point was reached, even when thin cracks were initiated in some of the walls.

The peak point is where the wall reached its ultimate loading capacity with little horizontal displacement. Then, the slope dropped rapidly, with noticeable change in strength and displacement, to a certain point based on the individual wall behavior. Afterwards, a steady decline was observed up to the end of the test as shown in Fig.8-a to Fig.8-d except for SF-r which could not sustain any further loading after the steep decline as shown in Fig.8-e.

3.3. Shear strength capacity of the walls

Walls GM-r and OG-r experienced initial cracks at about 85% of their peak loads and after their steep decline at peak loads, they experienced a

very gradual and steady slope decline in their post peak behavior as shown in Fig.8-b and d. The other walls did not initiate cracks until the peak load was reached.

It is important to note that high alkali environments present in mortar, as well as moisture and heat, can negatively impact the strength of a wild cane and cause deterioration [18]. Among the mesh strengthened walls (PM-r, GM-r, SM-r), SM-r, strengthened with steel mesh, had the highest strength recovery (89% of SM) along with the highest strength drop (70%) after the peak point as shown in Fig.8-c which suggests that the steel mesh used was not fully utilized for its ductility as demonstrated by the de-bonding failure.

This is probably due to the absence of bolt anchorages (rather than the wire ties) to anchor the mesh with the wall. Wall PM-r showed the least strength recovery (43%) out of all the walls but was able to add some ductility to the wall unlike SF-r which had a slightly higher strength recovery (47%) but did not change the brittle type failure and the post peak behavior of its original wall (SF) as shown in Fig.(8-a and e).

The residual or retained strength of the strengthened walls are due to the shear strength capacity of the wall due to the applied pre-compression after the slippage of the wall at the shear planes (bed joints). The strengthening keeps the cracks from widening to a large extent hence retaining the shear strength developed from frictional normal force.

3.4. Ductility of the tested walls

An important factor to be considered for analyzing masonry walls is ductility which establishes the deformation capacity of the walls beyond their elastic limits. A ductility factor μ, usually defined as the energy dissipation capacity of a wall [19], is the ratio between the displacement of a wall in its elastic and inelastic range. In this study, the chosen displacements are at 66% of the pre-peak load (for serviceability purposes) and at 33% of the post-peak load. These values establish a baseline for the tested walls in order to facilitate comparison.

Another factor relating to energy dissipation is toughness, which according to ASTM C 1018-97[20], can be obtained from the area under the load-displacement curve. This property gives us an indication of the energy absorption capability of the walls before collapsing.

The un-strengthened walls did not show any signs of ductility after their failure. The strengthened walls, on the other hand, were quite different in their post peak behavior. The ductility factor of GM-r (23.2) was the highest amongst the strengthened walls followed by OG-r (14.4) as summarized in Table (5). This shows that GM-r retained its strength and offered the highest ductility compared to the other strengthened walls since large displacements were attained before reaching 33% of its post peak strength. This is due to the high tensile strength of the glass fiber mesh and its efficient bond with the cement plaster However, upon further examination and looking at the ultimate deflection/first crack ratio Table 5 , wall OG-r exhibited the largest amounts of deformations but was not able to retain as much strength as GM-r due to the rupture of the wild cane.

Walls PM-r and OG-r also showed good ductility before finally succumbing to failure. Wall SF-r, in terms of ductility, was identical to the un-strengthened walls since it exhibited a sudden brittle failure.

This shows that the steel fiber was not utilized fully and thus it is not applicable in this field where repairing or strengthening is required. In terms of toughness, OG-r was about 10 times higher than its original wall (OG), which is the highest toughness value compared to the others as summarized in Table 6.

This is due to the initial high strength restoration of the material. However, GM-r had a lower post peak strength decline compared to OG-r, and thus a fairly high toughness ratio of 8.3.

It is possible that the spacing of the glass fiber mesh, as compared to the spacing of the organic grid, had a higher impact on the overall ductility of the wall. SM-r had a high toughness ratio (7.0) due to its high strength retention (89% of SM). However, due to its brittle de-bonding failure, it

cannot be dependable since its energy dissipation was very sudden.

4. Conclusions

The present study investigated the strengthening of previously damaged masonry brick walls under lateral in-plane loading with a pre-defined vertical compression load. From the experimental results, the following conclusions can be drawn.

1- All the un-strengthened walls failed in a sudden diagonal shear failure with no apparent ductility.
2- GM-r, strengthened with glass fiber mesh, had the highest ductility factor of 23.2 which shows the best strength retention amongst the strengthened walls. The glass fiber mesh reduced the effects of sudden failure by keeping the cement plaster and wall intact and restored the shear strength by 68%.
3- OG-r, strengthened with wild cane grid, had the highest toughness ratio value of 10.1 and the highest ultimate crack displacement of 54mm which shows the best energy absorption capability. The wild cane strip grid restored the shear strength integrity of the wall by 81% and increased ductility making it a fairly viable strengthening material. However, wild cane will not be a good option for walls that are prone to weathering effects such as exterior walls due to biological decay factor.
4- SM-r, strengthened with steel mesh, showed the highest shear strength restoration at 89%. However, its sudden de-bonding failure limits its ductility and makes it a bad choice as a strengthening material. The de-bonding failure could be fixed by bolt anchoring to the wall. Alternatively, larger spaced steel mesh could be used to take advantage of the ductile property of the steel by causing the steel mesh to yield or rupture.
5- PM-r, strengthened with plastic mesh, did not participate much in restoring the shear strength of the wall. However, it reduced the effect of the brittle failure making it more subtle and delayed the ultimate failure of the wall. Using high strength plastic mesh could potentially increase the shear strength and improve on the ductility factor of the damaged wall.
6- SF-r, strengthened with steel fibers, restored neither shear strength nor ductility of SF. The steel fibers only served to limit the surface cracks on the cement plaster when compared with the failure of PL (the cement plastered control wall). This material is not recommended as a strengthening material.

References

1- Mustafaraj, E., & Yardim, Y. (2018). In-plane shear strengthening of unreinforced masonry walls using GFRP jacketing. Periodica Polytechnica Civil Engineering, 62(2), PP. 330-336.
2- Rahman, A., & Ueda, T. (2016). In-plane shear strength of masonry wall strengthening by two distinct FRPs. Journal of Structural Engineering, A, 62, PP. 915-925.
3- Yardim, Y., & Lalaj, O. (2016). Shear strengthening of unreinforced masonry wall with different fiber reinforced mortar jacketing. Construction and Building Materials, 102, PP. 149-154.
4- Hrasnica, M., Biberkic, F., & Medic, S. (2017). In-plane behavior of plain and strengthened solid brick masonry walls. In Key Engineering Materials (Vol. 747, PP. 694-701).
5- Oskouei, A. V., Jafari, A., Bazli, M., & Ghahri, R. (2018). Effect of different retrofitting techniques on in-plane behavior of masonry wallettes. Construction and Building Materials, 169, PP. 578-590.
6- ElGawady, M. A., Lestuzzi, P., & Badoux, M. (2006). Retrofitting of masonry walls using shotcrete. In 2006 NZSEE Conference, Paper (Vol. 45).
7- Turco, V., Secondin, S., Morbin, A., Valluzzi, M. R., & Modena, C. (2006). Flexural and shear strengthening of un-reinforced masonry with FRP bars. Composites Science and Technology, 66(2), PP. 289-296.
8- Ismail, N., Petersen, R. B., Masia, M. J., & Ingham, J. M. (2011). Diagonal shear behaviour of unreinforced masonry wallettes strengthened using twisted steel bars. Construction and Building Materials, 25(12), PP. 4386-4393.
9- 10-9 Shabdin, M., Zargaran, M., & Attari, N. K. (2018). Experimental diagonal tension (shear) test of Un-Reinforced Masonry (URM) walls strengthened with textile reinforced mortar (TRM). Construction and Building Materials, 164, PP. 704-715.
10- Moroz, J. G., & Lissel, S. L. (2009). Tonkin cane bamboo as reinforcement in masonry shear walls. In 11th Canadian Masonry Symposium.
11- Menna, C., Asprone, D., Durante, M., Zinno, A., Balsamo, A., & Prota, A. (2015). Structural behaviour

تقوية مقاومة القص الجانبية للجدران بعد التضرر

أحمد محمد رؤوف[1] - طالب ماجستير
د . جلال أحمد سعيد[1] - استاذ

[1]جامعة السليمانية ، كلية الهندسة ، قسم الهندسة المدنية

المستخلص

تم دراسة تأثير خمسة أنواع مختلفة من مواد التقوية جدران طابوقية الأعادية تحت تأثير أحمال جانبية في مستوى الجدار. تم فحص سبعة جدران من الطابوق الطيني بأبعاد (1200 × 935 × 115) ملم ، وقد تم تحميل خمسة منها الى حد الفشل الأولي ومن ثم تقويتها بالمواد التالية ، التقوية بمشبك بلاستيكي ، مشبك من الألياف الزجاجية ، مشبك من الفولاذ ، مشبك من القصب المحلي ، وألياف فولاذية مقطعة ، و فحصها من جديد لحد الفشل لأجل دراسة خواصها من حيث مقاومة القص والمستمطلية. وقد بينت النتائج بأن الجدار المقواة بالألياف الزجاجية لها أكبر عامل استطالة (23.2) وأكبر مقاومة متبقية بعد التضرر من بين الجدران المقواة. والجدار المقواة بالقصب ألمحلي لها أكبر نسبة صلادة (10.1). الجدار المقواة بالمشبك الفولاذي أبقت على (89%) من مقاومة الأولية ولكنها غير صالحة لحالات التعرض للهزات الارضية بسبب فشلها المفاجئ عن طريق فصلها عن الجدار. أما الجدران المقواة بالمشبكات البلاستيكية والألياف الفولاذية المقطعة لم تستطيع استعادة مقاومتها أو استطالتها.

الكلمات المفتاحية : أحمال جانبية ، جدران كتل البناء ، جدران متضررة ، مقاومة القص ، مواد تقوية.

of masonry panels strengthened with an innovative hemp fibre composite grid. Construction and Building materials, 100, PP. 111-121.

12- Parisi, F., Iovinella, I., Balsamo, A., Augenti, N., & Prota, A. (2013). In-plane behaviour of tuff masonry strengthened with inorganic matrix–grid composites. Composites Part B: Engineering, 45(1), PP. 1657-1666.

13- Chagas, J. N., & Moita, G. F. (2016). Fibre Reinforced Polymers in the Rehabilitation of Damaged Masonry. Sustainable Construction (PP. 1-21).

14- Weng, D., Lu, X., Zhou, C., Kubo, T., & Li, K. (2004). Experimental study on seismic retrofitting of masonry walls using GFRP. In Proceedings of 13th World Conference on Earthquake Engineering (PP. 1-6).

15- ElGawady, M. A., Lestuzzi, P., & Badoux, M. (2005). In-plane seismic response of URM walls upgraded with FRP. Journal of Composites for Construction, 9(6), PP. 524-535.

16- Konthesingha, K. M. C., Masia, M. J., Petersen, R. B., Mojsilovic, N., Simundic, G., & Page, A. W. (2013). Static cyclic in-plane shear response of damaged masonry walls retrofitted with NSM FRP strips–An experimental evaluation. Engineering Structures, 50, PP. 126-136.

17- Santa-Maria, H., & Alcaino, P. (2011). Repair of in-plane shear damaged masonry walls with external FRP. Construction and Building Materials, 25(3), PP. 1172-1180.

18- Archila, H., Kaminski, S., Trujillo, D., Escamilla, E. Z., & Harries, K. A. (2018). Bamboo reinforced concrete: a critical review. Materials and Structures, 51(4), PP. 102.

19- Miha, T. (1999). Earthquake-resistant Design of Masonry Buildings (Vol. 1). Singapore: World Scientific.

20- ASTM C1018-97, Standard Test Method for Flexural Toughness and First-Crack Strength of Fiber-Reinforced Concrete (Using Beam With Third-Point Loading), ASTM International, West Conshohocken, PA, 1997.

21- Iraqi Standards IQS No. 24/1988.

22- ASTM C1314-03, Standard Test Method for Compressive Strength of Masonry Prisms, ASTM International, West Conshohocken, PA, 2003.

23- ASTM C109 / C109M-02, Standard Test Method for Compressive Strength of Hydraulic Cement Mortars (Using 2-in. or [50-mm] Cube Specimens), ASTM International, West Conshohocken, PA, 2002.

24- ASTM C307-03, Standard Test Method for Tensile Strength of Chemical-Resistant Mortar, Grouts, and Monolithic Surfacings, ASTM International, West Conshohocken, PA, 2003.

25- ASTM C348-02, Standard Test Method for Flexural Strength of Hydraulic-Cement Mortars, ASTM International, West Conshohocken, PA, 2002.

26- British Standards Institution. (2009). BS EN 12390-3:2009 – Testing hardened concrete. Milton Keynes.

Table 1: Description of the walls with their strengthening materials. (Source: Researcher)

No.	Specimen		Type of strengthening
	Designation	Description	
1	C	Control wall	None; plain wall used as reference
2	PL	Plastered control wall	None; Cement plastered (C.P) wall used as reference for C.P. walls
3	PM-r	Plastic Mesh	Plastic polypropylene mesh w/C.P
4	GM-r	Glass Mesh	Glass fiber mesh w/C.P
5	SM-r	Steel Mesh	Small diameter welded wire steel mesh w/C.P
6	OG-r	Organic Grid	Cane strips in orthogonal directions w/C.P
7	SF-r	Steel Fiber	0.5 mm diameter manually chopped steel fiber w/C.P

Table 2: Mechanical properties of the materials. (Source: Researcher)

Materials	Compressive strength (MPa)	Tensile strength (MPa)	Flexural strength (MPa)	Specification
Brick	28.39	*	8	IQS No. 24 [21]
Brick prism	38.39	*	*	ASTM C1314-03 [22]
Masonry mortar (1:3)	45.37	3.12	9.48	
Cement plaster mortar (1:3)	36.51	*	*	ASTM C109-02 [23] ASTM C307-03 [24]
S.F. cement plaster mortar (1:3)	49.11	3.7	8.8	ASTM C348-02 [25]
Crack repair mortar (1:2)	55.52	3.07	*	
Concrete cubes	37.52	*	*	BS EN 12390-3 [26]

Table 3: Mechanical properties of the strengthening materials. (Source: Researcher)

Strengthening Material	Ultimate tensile strength (MPa)	Weight
Plastic mesh	17.3	223 g/m^2
Glass fiber mesh	238.7	88 g/m^2
Steel mesh	303	2257 g/m^2
Wild cane	94	58 g/m (length)
Steel fiber	418	1.5% by mortar volume

Table 4: Test result of the specimens. (Source: Researcher).

Wall	Peak load (kN)		Peak load of strengthened / peak load of original (%)
	Original wall	Strengthened wall	
C	254.3	*	*
PL	269.2	*	*
PM-r	314.1	134.6	43
GM-r	209.4	142.1	68
SM-r	284.2	254.3	89
OG-r	239.3	194.4	81
SF-r	284.2	134.6	47

Table 5: Ductility factor and displacement values of the walls. (Source: Researcher)

Wall	$\delta_{66\%}$ pre-peak (mm)	$\delta_{33\%}$ post-peak (mm)	$\delta_{33\%}$ post-peak / $\delta_{66\%}$ pre-peak	First crack displacement (mm)	Peak crack displacement (mm)	Ultimate crack displacement (mm)	Ultimate / first crack displacement
C	*	*	*	4.8	4.8	4.8	1.0†
PL	*	*	*	6.0	6.0	6.0	1.0†
PM-r	1.4	15.2	10.6	2.2	2.2	16.7	7.5
GM-r	1.5	34.5	23.2	2.1	4.3	38.7	18.3
SM-r	3.9	17.3	4.4	6.3	9.3	31.2	4.9
OG-r	1.9	27.7	14.4	2.3	2.7	54.0	23.2
SF-r	*	*	*	3.6	3.6	3.6	1.0†

† The ultimate crack and the first crack are the same due to the explosive sudden failure.

Table 6: Toughness values of the walls. (Source: Researcher)

Wall	Toughness of original wall (N.m)	Toughness (N.m)	Toughness ratio with original wall
	*	624.4	*
C	*	688.4	*
PL	733.3	1238.0	1.7
PM-r	338.9	2825.8	8.3
GM-r	524.2	3663.4	7.0
SM-r	410.9	4149.3	10.1
OG-r	661.3	231.8	0.4

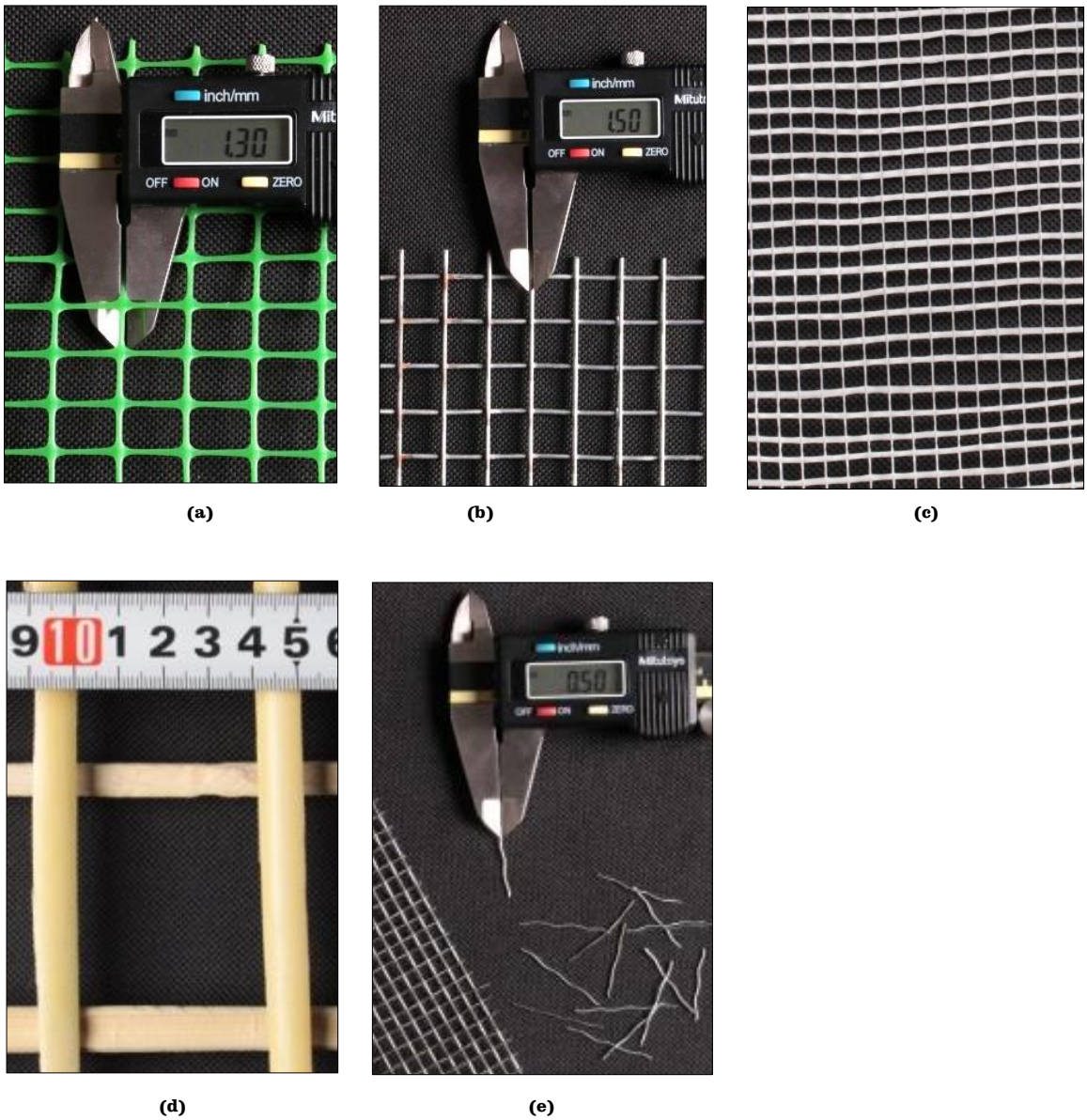

(a) **(b)** **(c)**

(d) **(e)**

Fig.1: Strengthening materials. (Source: Researcher)

(a) plastic mesh.

(b) steel mesh.

(c) glass fiber mesh.

(d) wild cane grid.

(e) Chopped steel fibers.

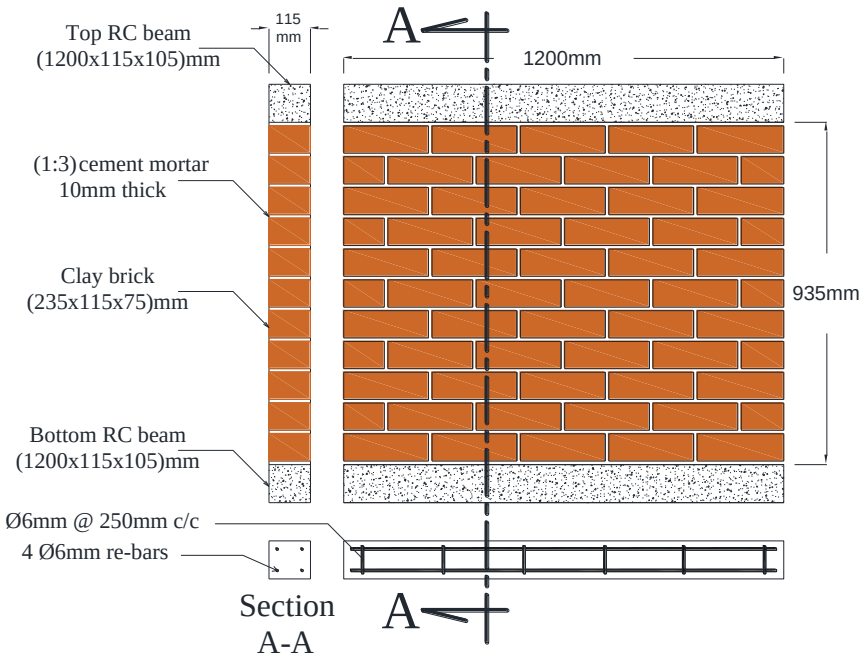

Fig.2: Detail of the tested specimen. (Source: Researcher)

(a) **(b)**

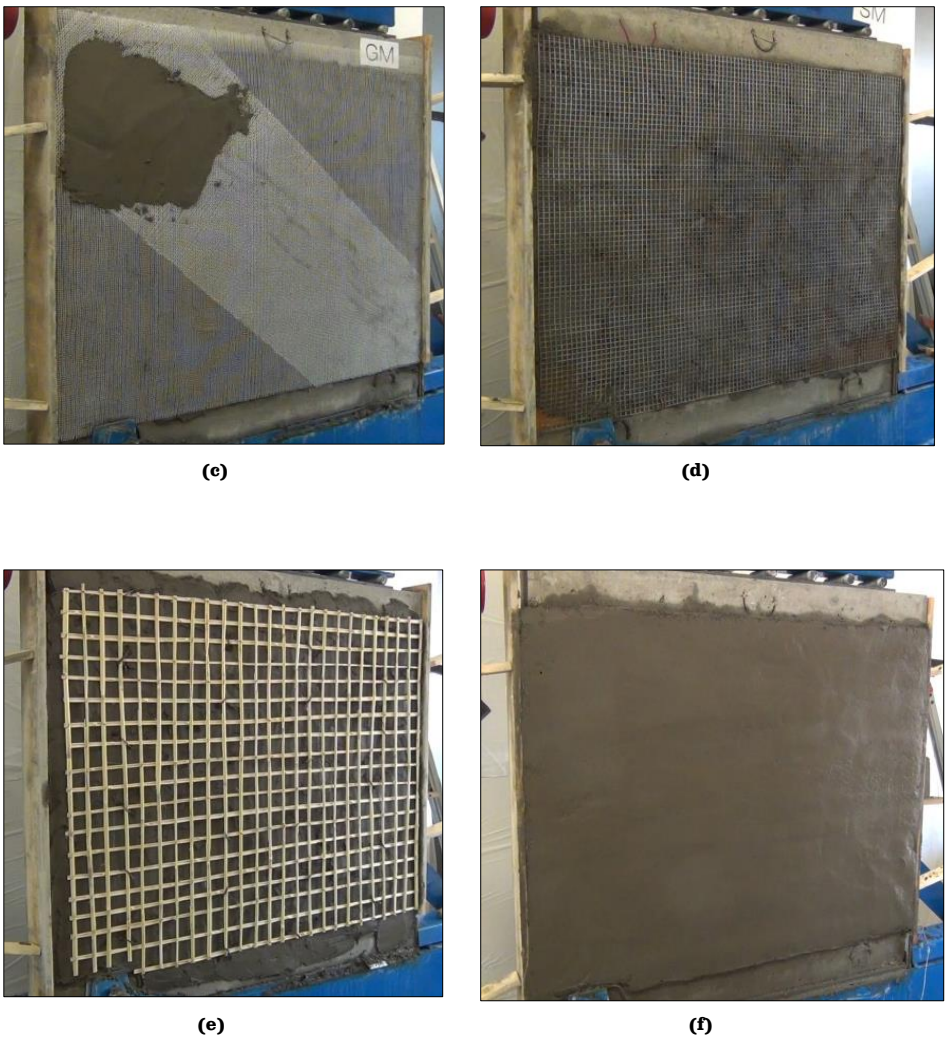

(c) **(d)**

(e) **(f)**

Fig.3: Strengthening procedure; (Source: Researcher)

(a) repairing initial damaged wall with 1:2 cement mortar.

(b) plastic mesh.

(c) glass fiber mesh.

(d) steel mesh.

(e) organic (wild cane) grid.

(f) steel fiber cement plaster.

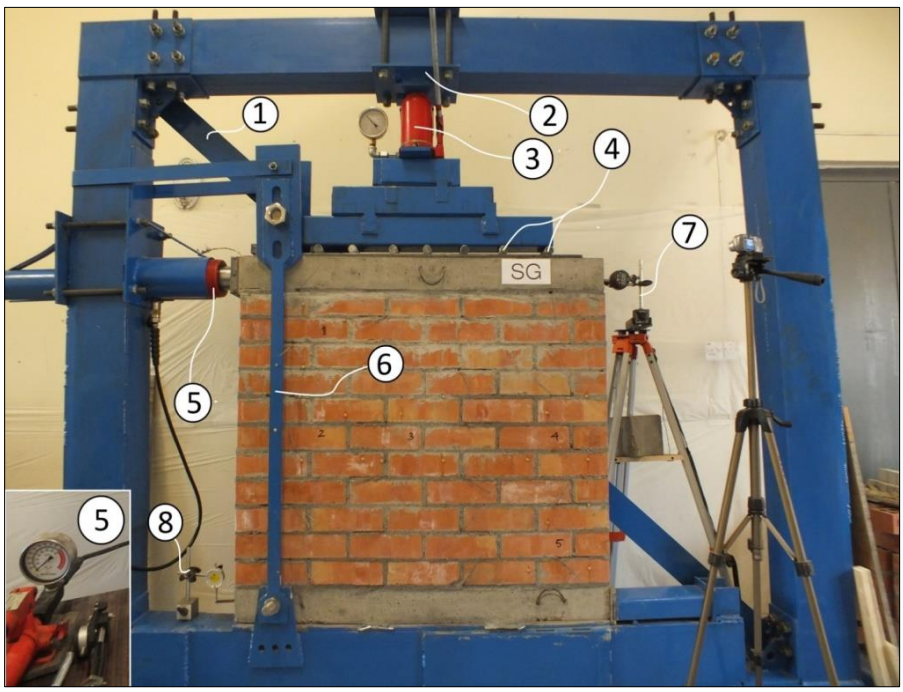

1- Diagonal steel rectangular plate (15 × 100)mm.
2- Steel plate (300 × 400 × 10)mm to hold the jacks in place.
3- Vertical jack with 30 Ton capacity.
4- Round bars to distribute the load and allow horizontal movement of the wall.
5- Lateral jack with 50 Ton capacity.
6- Vertical link (40 × 15)mm at front and back.
7- A digital dial gauge with 0.001mm accuracy to measure horizontal movement.
8- A dial gauge with 0.01mm accuracy to measure vertical movement.

Fig.4: Detail of the testing frame. (Source: Researcher)

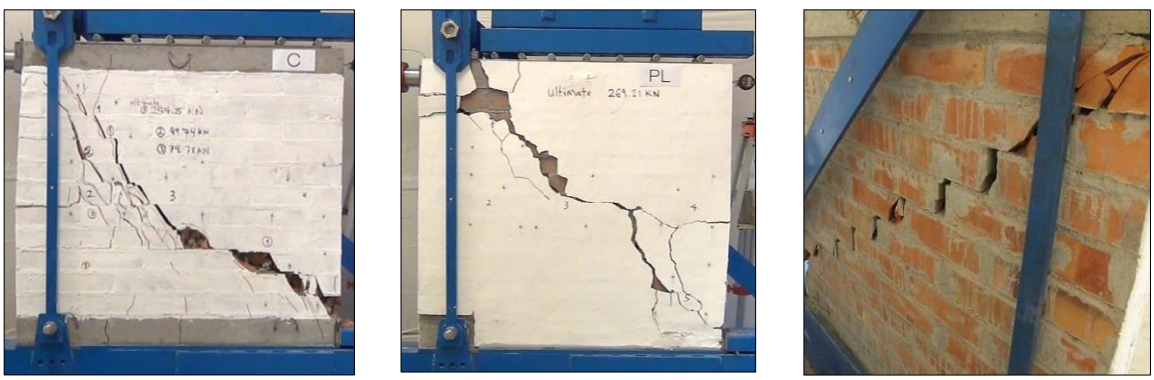

(a) **(b)** **(c)**

Fig 5: Failure mechanism of the control walls; (Source: Researcher)
(a) plain wall "C"
(b) front side of cement plastered wall "PL"
(c) backside of cement plastered wall "PL".

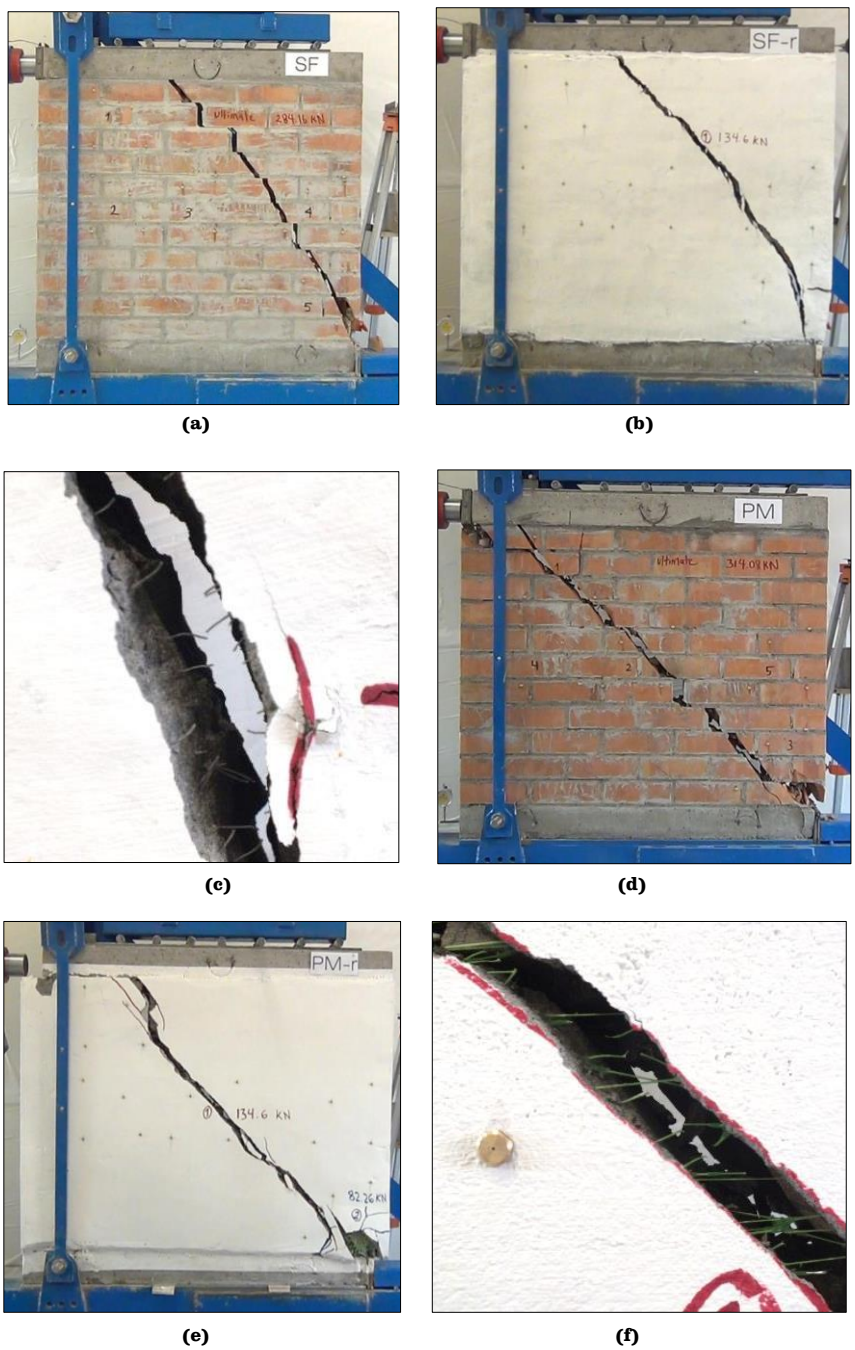

(a) **(b)**

(c) **(d)**

(e) **(f)**

Fig.6: Failure mechanism of tested un-strengthened and strengthened walls; (a) wall SF(b) wall SF-r, (c) steel fiber separation, (d) wall PM (e) wall PM-r, (f) elongation and rupture of plastic mesh strands. (Source: Researcher)


GM
1
2
3
4

(a)

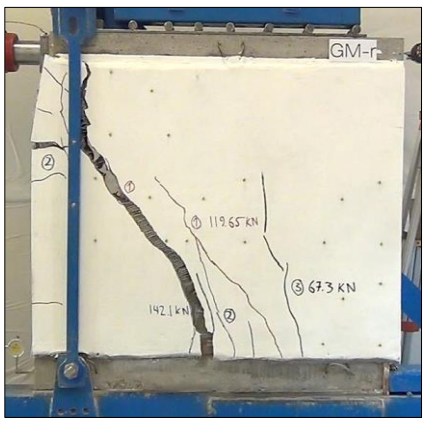
GM-r
① 119.65 KN
③ 67.3 KN
142.1 KN
②

(b)

(c)

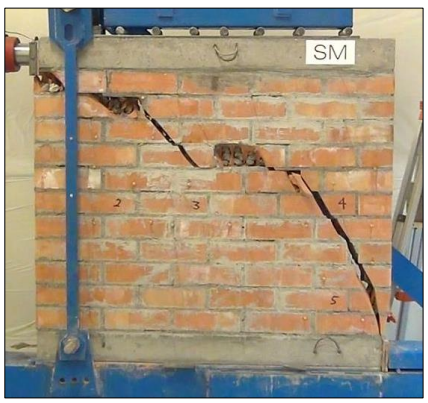
SM
2
3
4
5

(d)

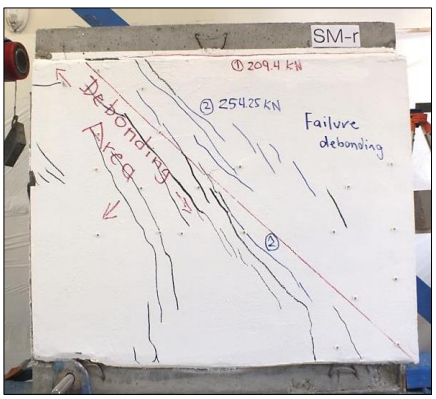
SM-r
① 209.4 KN
② 254.25 KN
Failure debonding
Debonding Area
②

(e)

(f)

(g) **(h)**

(i) **(j)**

Fig.7: Failure mechanism of tested un-strengthened and strengthened walls; (Source: Researcher)
(a) wall GM
(b) wall GM-r.
(c) plain side of GM-r .
(d) wall SM (e) wall SM-r.
(f) cement plaster de-bonding of wall SM-r.
(g) plain side of SM-r .
(h) wall OG.
(i) wall OG-r.
(j) plain side of wall OG-r.

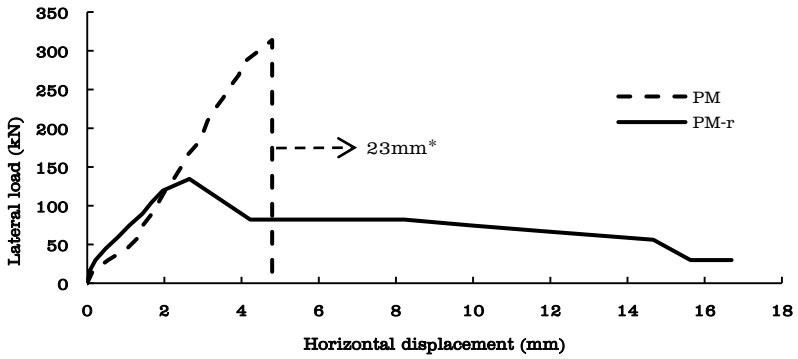
Lateral load (kN)
Horizontal displacement (mm)
PM
PM-r
23mm*

(a)

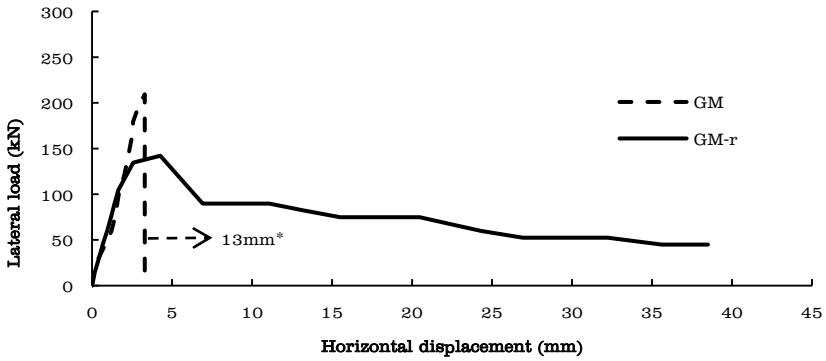
Lateral load (kN)
Horizontal displacement (mm)
GM
GM-r
13mm*

(b)

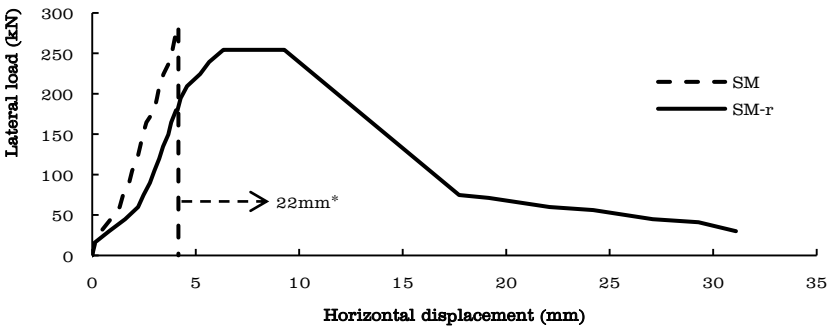
Lateral load (kN)
Horizontal displacement (mm)
SM
SM-r
22mm*

(c)

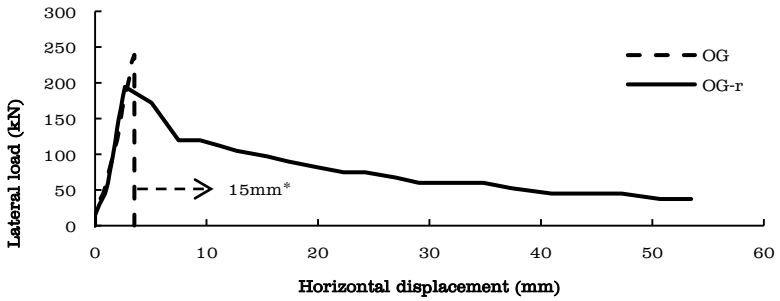

(d)

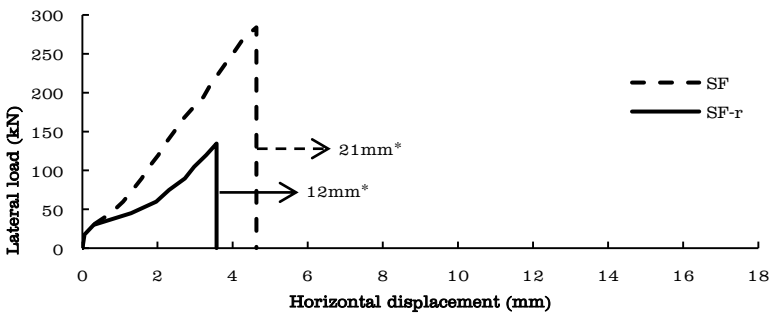

(e)

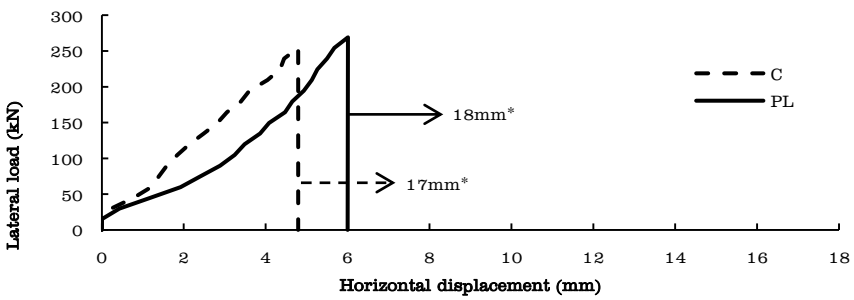

(f)

* Represents the obtained displacement after the sudden failure.

Fig.8: Load displacement graphs for the tested walls before after strengthening with the following; (a) plastic mesh (b) glass fiber mesh (c) steel mesh (d) wild cane grid (e) chopped steel fiber (f) test results of the plain "C" and cement plastered "PL" control walls. (Source: Researcher)